Applied Chemical Engineering (2021) Volume 4 Issue 2
doi:10.24294/ace.v4i2.1357

ORIGINAL RESEARCH ARTICLE

Photocatalytic degradation of ammonia-nitrogen via N-doped graphene/bismuth sulfide catalyst under near-infrared light irradiation

Wenxiao Liu[1,2], Shouqing Liu[1,2*]

[1] *School of Chemistry, Biology and Materials Engineering, Suzhou University of Science and Technology, Suzhou 215009, China. E-mail: shouqing_liu@163.com*

[2] *Jiangsu Key Laboratory of Environmental Functional Materials, Suzhou 215009, China*

ABSTRACT

The N-doped graphene/bismuth sulfide (NG/Bi_2S_3) composite was synthesized by hydrothermal method. The structure and properties of the catalyst were characterized by X-ray powder diffraction, Raman spectroscopy, scanning electron microscopy and UV-visible near-infrared diffuse reflectance spectroscopy. The degradation of ammonia-N was studied using 0.050 g NG/Bi_2S_3 as photocatalyst under near-infrared light irradiation. The results show that the degradation ratio of ammonia-N reaches 91.4% in 100.0 $mg \cdot L^{-1}$ ammonia-N solution with pH 9.0 under near-infrared light irradiation for 10 h. Under similar conditions, the degradation ratio of ammonia-N is only 65.5% when pure Bi_2S_3 is used as the photocatalyst. Kinetic studies show that the ammonia-N degradation follows the first-order reaction kinetics, and the average value of the apparent rate constant is 0.1240 h^{-1}. Catalyst stability studies show that the degradation ratio of ammonia nitrogen in 7 runs is still greater than 85.5%, which indicates that the NG/Bi_2S_3 composite catalyst is very stable.

Keywords: NG/Bi_2S_3; Near-infrared; Photocatalysis; Ammonia Nitrogen; Degradation

ARTICLE INFO

Received: 16 August 2021
Accepted: 6 October 2021
Available online: 12 October 2021

1. Introduction

Ammonia nitrogen (NH_4^+/NH_3) has become a major pollutant in water bodies. Industrial sewage, garbage leachate contains a large amount of ammonia nitrogen[1,2]. When the ammonia concentration is too large, it can cause harm to the organisms in the water[3]. The World Health Organization recommends that the total amount of ammonia nitrogen in drinking water should not exceed 1.5 $mg \cdot L^{-1}$[4,5]. With the continuous progress of photocatalytic technology, it has become possible to degrade ammonia nitrogen by using near-infrared photocatalysis.

Bismuth sulphide (Bi_2S_3) is a semiconductor catalyst with a near-infrared light response. Its band width is approximately 1.3 eV. The catalyst has good prospect in thermal power[6], photovoltaic cells and flexible solar cells[7]. The Bi_2S_3 lattice belongs to an orthogonal crystal line. It is anisotropic and easy to form crystal structures with high aspect ratio under suitable growth conditions[8]. Its synthetic products mainly include nanowire[9], nanorods[10], nanodisk[11], etc. Because aza-graphene (NG) can improve its catalytic activity after compounding with photocatalyst[12–16], Bi_2S_3 is synthesized by hydrothermal method, and then NG is loaded on Bi_2S_3 to form NG/Bi_2S_3 composite pho-

tocatalyst, and the degradation of the performance of the photocatalyst under near-infrared light was investigated.

2. Experiment

2.1 Drug

Graphite powder was purchased at Shanghai Colloidal Chemical Factory. $Bi(NO_3)_3·5H_2O$ was purchased from Sinopharm Chemical Reagent Co., Ltd. NaOH, thiourea and $KMnO_4$ were all purchased from Shanghai Reagent General Factory, China. NH_4Cl was purchased from Cangzhou Tengcheng Chemical Products Co., Ltd. H_2O_2 was purchased from Wuxi Zhanwang Chemical Co., Ltd. Concentrated H_2SO_4 was purchased from Kunshan Dongmei Chemical Co., Ltd.

2.2 Preparation of graphene oxide

Graphene oxide (GO) was synthesized by improved Hummers method[17]. Accurately weigh 3.0 g of graphite powder and wash with 10% dilute hydrochloric acid twice, then wash it with deionized water to neutral, and dry it at 60 ℃ for 12 h. Firstly, accurately weigh 1.0 g of cleaned graphite powder into a 500 mL beaker and place it into the water bath and stir continuously at low temperature (<5 ℃). Secondly, 15.0 mL concentrated sulfuric acid was accurately added to the suspension of graphite powder, and magnetic stirring was carried out for 30 min. 3.0 g potassium permanganate was accurately weighed, and slowly added to the mixture, stirring for 30 min, controlling the temperature not to exceed 20 ℃. Take an accurate amount of 45 mL deionized water, slowly drop into the mixture, and stir continuously for 30 min. Finally, hydrogen peroxide solution (10%, 150 mL) was added slowly and stirred at room temperature for 24 h. Stand still, wash to neutral, take the lower mixture and dry it in a 60 ℃ vacuum drying oven for 24 hours to obtain GO.

2.3 Preparation of aza-graphene

Accurately weigh 70 mg GO and disperse it in 50 mL of deionized water by ultrasound. Accurately weigh 21.0 g of urea and add it to the above solution, mix it evenly, add water to 70 mL, dissolve it by ultrasound for 60 min, then transfer it to a high-pressure hydrothermal reactor, and heat it tightly at 170 ℃ for 12 h. After the sample is cooled to room temperature, it is washed and filtered with deionized water and dried in a 60 ℃ vacuum drying oven for 24 hours to obtain NG.

2.4 Preparation of the NG/Bi_2S_3

Accurately weigh 0.6 g $Bi(NO_3)_3·5H_2O$ (1.24 mmol) and disperse it in 20.0 mL deionized water by ultrasound. Weigh 15.9 mg NG(Bi_2S_3 5 wt%) and slowly add it to the above solution for ultrasonic dispersion for 30 min. Accurately weigh 0.188 g (2.48 mmol) of thiourea, dissolve it in 20 mL of deionized water, slowly drop it into the above suspension, and continue stirring for 3 h. Accurately measure 10 mL NaOH (1 $mol·L^{-1}$), slowly add it to the above solution, and continue stirring for 2 h. Finally, the total volume of the solution is controlled at about 60 mL. The suspension is transferred to a 100 mL stainless steel autoclave, heated to 150 ℃ in the oven and maintained for 14 h. Cool the sample naturally to room temperature, then wash, filter and dry it in a 60 ℃ vacuum drying oven for 24 h to obtain NG/Bi_2S_3 hybridization photocatalyst. Similarly, Bi_2S_3 can be prepared.

2.5 Characterization of catalyst

The crystal phase structure of the catalyst was characterized by X-ray powder diffraction (XRD, X-ray powder diffractometer, model: D8/DISCOVE, Brooke Company, Germany). The X-ray source is Cu-Kα. The radiation wavelength is 0.154 nm, and the tube voltage and tube current are 40 kV and 40 mA respectively. Scanning electron microscope (SEM, scanning electron microscope, model: TecnaiG220, American FEI company) is used to characterize the morphology and particle size of the catalyst. The diffuse reflectance spectra of the samples were measured by UV-Vis diffuse reflectance spectroscopy (UV-Vis DRS, UV-Vis diffuse reflectance spectrometer, model: Shimadzu UV 3600 plus, Shimadzu company, Japan). The Raman spectra of the samples were measured under 633 nm laser

excitation (Raman spectrometer, model: LabRam HR800, HORIBA Jobin Yvon Company, France).

2.6 Photocatalytic degradation assay

LED lamps with wavelength of 850 nm were used as a light source. The degradation of ammonia nitrogen was carried out in a 100 mL glass beaker with a cooling device, surrounded by tin foil, and the distance between the light source and the ammonia nitrogen solution is approximately 15 cm. The concentration of ammonia nitrogen was 100 mg·L^{-1}, volume was 50 mL and the catalyst amount was 0.050 g. 0.1 mol·L^{-1} $NaHCO_3$-Na_2CO_3 buffer solution was used to control the reactor solution pH value.

Under magnetic stirring, the reactor containing the reaction mixture was placed under near-infrared light. Determine the content of ammonia nitrogen in the reaction solution by Nessler's reagent method[18]: take 1.0 mL of ammonia nitrogen reaction solution every 1 h, put it into the colorimetric tube, add deionized water to 48 mL, add 1.0 mL of potassium sodium tartrate and 1.0 mL of Nessler's reagent, mix and shake, stand still for 10 min, and determine the absorbance of ammonia nitrogen reaction solution by ultraviolet visible spectrophotometer.

The maximum absorbance of the hourly ammonia nitrogen reaction solution was measured according to the above method. Referring to Lamberbill's law, the ammonia nitrogen concentration is positively proportional to the absorbance within a certain range of concentrations.

$$\eta_{degradation\ rate\ of\ NH_4^+/NH_3} = \left(1 - \frac{C_i}{C_0}\right) \times 100\% = \left(1 - \frac{A_i}{A_0}\right) \times 100\%$$

Among them, C_0 is the initial concentration of ammonia nitrogen. A_0 is the absorbance of the initial solution. C_i is the concentration of the remaining ammonia nitrogen, and A_i is the absorbance of the remaining ammonia nitrogen.

3. Results and discussion

3.1 X-ray powder diffraction characterization

Figure 1 shows the XRD diffraction patterns of NG, Bi_2S_3 and NG/Bi_2S_3. The diffraction surface corresponding to each diffraction peak is shown in **Table 1**, which is consistent with the spectrum of standard card JCPDS 17–0320. Comparing curves **Figure 1(b)** and **Figure 1(c)**, it can be seen that the diffraction pattern of NG/Bi_2S_3 is basically consistent with Bi_2S_3. At the same time, the diffraction peak of (002) plane of NG at 26.2° is observed in the diffraction pattern of NG/Bi_2S_3, indicating that NG and Bi_2S_3 form a complex substance.

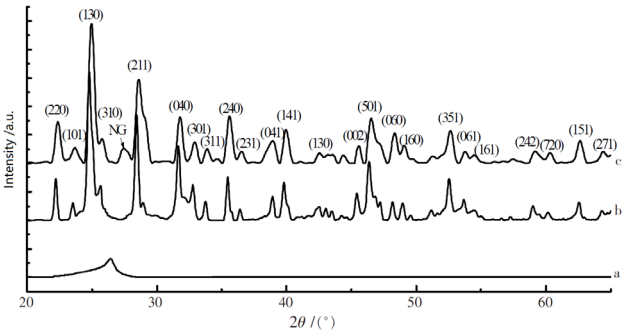

Figure 1. XRD patterns (a. NG, b. Bi_2S_3, c. NG/Bi_2S_3).

Table 1. Results of the XRD analysis of the Bi_2S_3 samples

2θ/(°) (hkl)	2θ/(°) (hkl)	2θ/(°) (hkl)	2θ/(°) (hkl)	2θ/(°) (hkl)	2θ/(°) (hkl)	2θ/(°) (hkl)
22.39 (220)	28.61 (211)	33.92 (311)	39.89 (141)	46.66 (501)	52.62 (351)	62.59 (171)
23.72 (101)	31.66 (040)	35.58 (240)	42.40 (241)	48.27 (060)	53.78 (061)	64.42 (271)
24.93 (130)	32.94 (301)	39.05 (041)	45.54 (002)	49.01 (160)	59.09 (242)	

3.2 Catalyst topography characterization

Figure 2 is the SEM image of NG, Bi_2S_3 and NG/Bi_2S_3 samples. It can be seen from **Figure 2(A)**, that NG is a two-dimensional layered structure. In **Figure 2(B)**, it can be observed that Bi_2S_3 is about 3 –5 μm in length. A rod structure with a radius isabout 20–30 nm. In **Figure 2(C)**, it can be clearly observed that Bi_2S_3 particles are well dispersed on the surface of NG, indicating that Bi_2S_3 and NG are well combined.

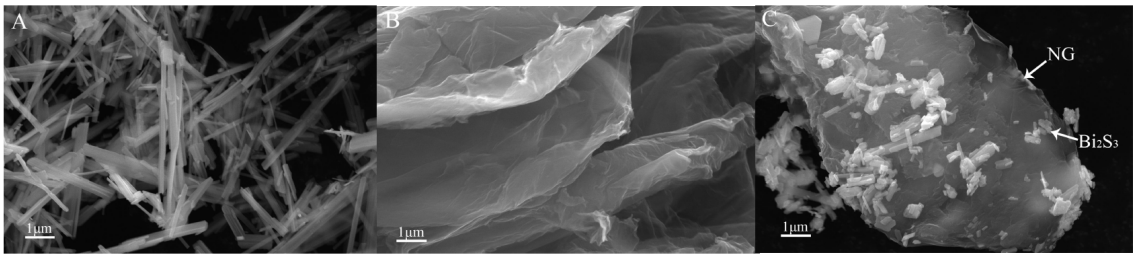

Figure 2. SEM spectrum (**A**. NG, **B**. Bi_2S_3, **C**. NG/Bi_2S_3).

3.3 Raman spectral characterization

Figure 3 is the Raman spectra of NG, Bi_2S_3 and NG/Bi_2S_3. As can be seen from **Figure 3**, 112.4 and 238.9 cm^{-1} are the two characteristic peaks of Bi_2S_3[19]. Two characteristic peaks can be observed at 1,567 cm^{-1} and 1,334 cm^{-1}, respectively, representing the G-band and D-band of graphene, of which 1,567 cm^{-1} (G-band) is the E_{2g} vibration mode of graphene, and 1,334 cm^{-1} (D-band) is caused by the defects and irregular structure of graphite structure[20,21]. It can be seen from **Figure 3** that the Raman peaks of Bi_2S_3 and NG are well combined, which further confirms the existence of NG in Bi_2S_3 composite catalyst.

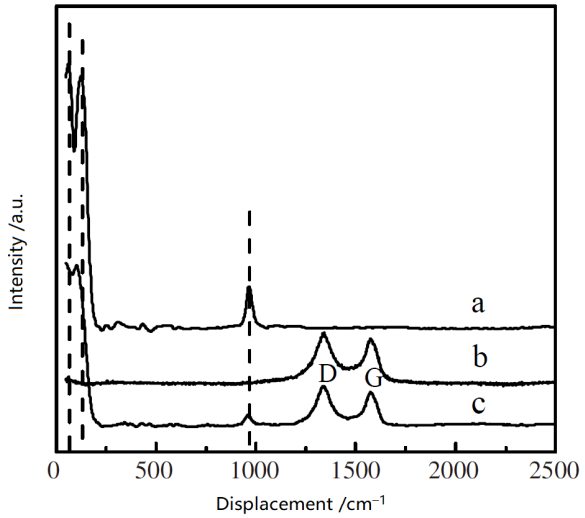

Figure 3. The Raman spectra (**a**. Bi_2S_3, **b**. NG, **c**. NG/Bi_2S_3).

3.4 Near-infrared diffuse spectra visible from the UV

Figure 4 shows the UV-VIS-NIR diffuse reflectance spectra of Bi_2S_3 and NG/Bi_2S_3 samples. It can be seen from **Figure 4** that the absorption of Bi_2S_3 is enhanced in the near infrared region. Comparing curve (a) and curve (b) in **Figure 4**, it can be found that Bi_2S_3 has absorption red shift after doping NG. Based on UV-VIS-INF-DRS spectrum, according to Tauc[22] equation, the direct band gaps of Bi_2S_3 and NG/Bi_2S_3 can be calculated.

$$(\alpha h\nu)^n = (Ah\nu - Eg)$$

In the formula, A is the constant of the semiconductor material; h is the Planck constant, ν is the frequency of light; α is the light absorption coefficient, Eg is the forbidden band width of the semiconductor, and $n = 2$ is the direct band gap.

Figure 5 are the two Tauc curves calculated from the data in **Figure 4**, with the direct band gap values for Bi_2S_3, NG/Bi_2S_3 of 1.32 eV and 1.29 eV, respectively. This means that after doping with NG, the Bi_2S_3 band width is reduced. Therefore, after the addition of NG, the absorption efficiency of incoming light can be effectively improved to improve the utilization of sunlight.

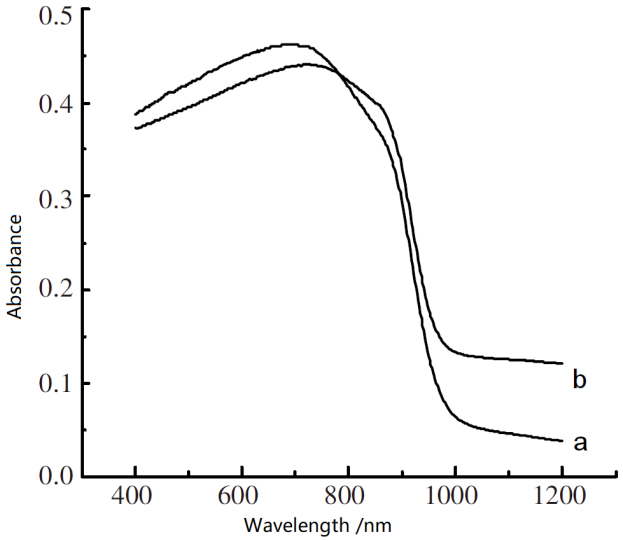

Figure 4. UV-visible-near-infrared light diffuse spectrum (**a**. Bi_2S_3, **b**. NG/Bi_2S_3).

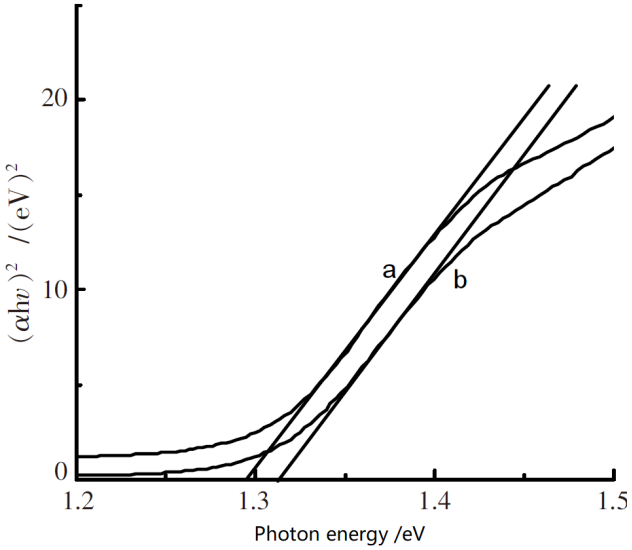

Figure 5. $(\alpha h\nu)^2$ and hν curve (**a**. Bi_2S_3, **b**. NG/Bi_2S_3).

3.5 Photocatalytic degradation of ammonia nitrogen experiment

3.5.1 Degradation of ammonia nitrogen under near-infrared light

The photocatalytic activities of Bi_2S_3 and NG/Bi_2S_3 were studied under different reaction conditions. In **Figure 6**, take 0.050 g NG/Bi_2S_3 as the catalyst to prepare 50 mL ammonia nitrogen solution with an initial concentration of 100 mg·L^{-1}, adjust the pH value of the water body to 9.0, and the degradation rate can reach 91.4% after 10 h. As shown in curve (b), 0.05 g Bi_2S_3 was used as catalyst, and the degradation rate reached only 65.5% after 10 h under similar conditions. This shows that the addition of NG enhances the catalytic activity of Bi_2S_3. Curve (c) shows that the ammonia nitrogen removal rate is only 22.3% after 10 h without light. Curve (d) shows that the volatilization rate of ammonia nitrogen is only 10% even when there is near-infrared light without catalyst. In conclusion, NG/Bi_2S_3 can effectively degrade ammonia nitrogen under near-infrared light radiation.

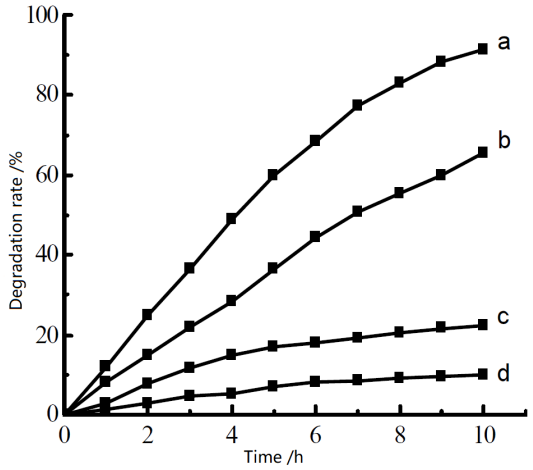

Figure 6. Near-infrared photocatalytic degradation of ammonia nitrogen curve.
Note: Degrading conditions: the solution volume V = 50 mL, and the initial concentration of ammonia nitrogen C = 100 mg·L^{-1}, pH = 9.0. **a**. 0.050 g NG/Bi_2S_3 + Near-infrared light; **b**. 0.050 g Bi_2S_3 + Near-infrared light; **c**. 0.050 g NG/Bi_2S_3 Empty-Illumination; **d**. Only Near-infrared light, without catalyst.

3.5.2 Effect of pH value on the degradation of ammonia nitrogen

Figure 7 shows the effect of pH on photocatalytic degradation of ammonia nitrogen. The degradation rate of ammonia nitrogen with pH value from 7.0 to 10.5 was investigated. When the pH of the solution is 7.0, the degradation rate of ammonia nitrogen is 10.0% after 10 hours of reaction. When the solution pH = 8.0, the degradation rate of ammonia nitrogen increased to 22.4%. When the pH value of the solution continued to increase to 9.0, the ammonia nitrogen degradation efficiency reached the highest value of 91.3%. Then, with the increase of pH value of the solution, the degradation rate of ammonia nitrogen decreased slightly, which were 81.0%, 76.6% and 72.4% respectively. This is because NH_4^+ is ionized with the increase of pH, and the concentration of NH_3 will increase with the increase of pH[23], which is conducive to the adsorption of NH_3 on the catalyst surface. When the pH of the solution is >9.0, competitive adsorption of OH^- may occur, which reduces the adsorption amount of ammonia nitrogen on the catalyst surface, resulting in the decline of degradation efficiency.

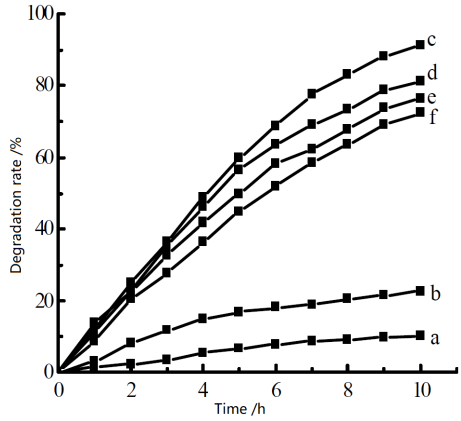

Figure 7. Effect of pH value on the degradation rate of ammonia nitrogen.
Note: Degradation conditions: in near-infrared light, the solution volume is V = 50 mL, and the initial concentration of ammonia nitrogen is C = 100 mg·L^{-1}, NG/Bi_2S_3 of mass m = 0.050 g. **a**. pH = 7.0; **b**. pH = 8.0; **c**. pH = 9.0; **d**. pH = 9.5; **e**. pH = 10.0; **f**. pH = 10.5.

3.5.3 Effect of the catalyst dosage on the degradation of ammonia nitrogen

Take a certain amount of NG/Bi_2S_3 catalyst and degrade the ammonia nitrogen solution with an initial concentration of 100 mg·L^{-1} under near-infrared light, as shown in **Figure 8**.

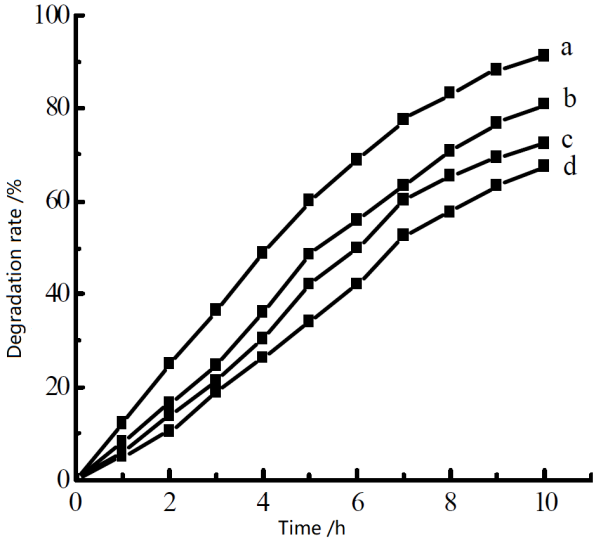

Figure 8. Effect of the catalyst dosage on the degradation rate of ammonia nitrogen.
Note: Degradation conditions: in near-infrared light, the solution volume is V = 50 mL, and the initial concentration of ammonia nitrogen is C = 100 mg·L^{-1}, pH = 9.0. **a**. 0.050 g; **b**. 0.10 g; **c**. 0.15 g; **d**. 0.20 g.

It can be seen from the curve in the figure that when the amount of catalyst is 0.050 g, the degradation rate of ammonia nitrogen reaches the best value. When the amount of catalyst increased from 0.050 g to 0.20 g, the efficiency of ammonia nitrogen degradation decreased gradually. Too much catalyst may lead to uneven dispersion and agglomeration of catalyst, thus affecting the contact between catalyst and solution and reducing catalytic activity.

3.5.4 Effect of NG doping on ammonia nitrogen degradation

Figure 9 shows the effect of NG content in the catalyst on photocatalytic degradation of ammonia nitrogen. The percentage of NG increased from 0.0% to 9.0%. In the initial stage, with the increase of NG content, the ammonia nitrogen degradation rate increased continuously. When NG increased to 3.0%, the ammonia nitrogen degradation rate reached the maximum value of 91.4%. When the content of NG exceeds 3.0%, the efficiency of ammonia nitrogen degradation is decreasing.

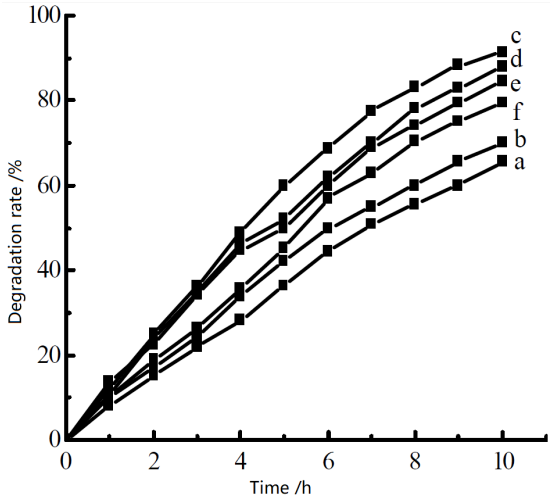

Figure 9. Effect of NG content on the degradation rate of ammonia nitrogen.
Note: Degradation conditions: in near-infrared light, solution volume V = 50 mL, initial concentration of ammonia nitrogen C = 100 mg·L^{-1}, pH = 9.0, and mass of NG/Bi_2S_3 is 0.050 g. **a**. 0%; **b**. 1.0%; **c**. 3.0%; **d**.5.0%; **e**. 7.0%; **f**. 9.0%.

3.5.5 Study on reaction kinetics

Changing the initial concentration of ammonia nitrogen, the degradation curve of ammonia nitrogen is shown in **Figure 10**. The analysis shows that $\ln(C_0/C_t)$ has a linear relationship with the reaction time t, as shown in **Figure 11**. Therefore, the ammonia nitrogen degradation reaction follows the first-order reaction kinetic equation. The average value of

apparent reaction kinetic rate constant K_{app} is 0.1240 h^{-1}.

$$\ln(C_0/C_t) = K_{app}t + b$$

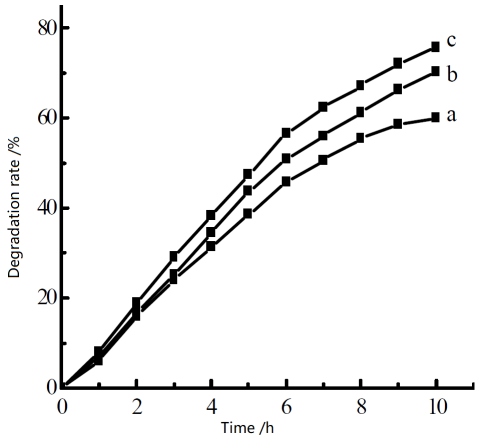

Figure 10. Effect of ammonia nitrogen concentration on the degradation rate of ammonia nitrogen.
Note: Degradation conditions: solution volume V = 50 mL, pH = 9.0, and mass of NG/Bi_2S_3 is 0.050 g. **a**. 5 mg·L^{-1}; **b**. 50 mg·L^{-1}; **c**. 75 mg·L^{-1}.

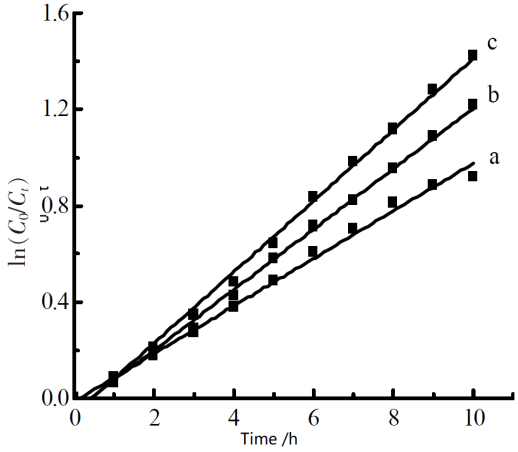

Figure 11. The relationship between $\ln(C_0/C_t)$ and time t at different initial ammonia nitrogen concentration. (**a**. 25 mg·L^{-1}; **b**. 50 mg·L^{-1}; **c**. 75 mg·L^{-1}).

3.5.6 Stability of catalyst

In order to evaluate the stability of the catalyst, cyclic catalytic experiments were carried out on the composite catalyst. The NG/Bi_2S_3 0.050 g composite catalyst was placed in the 50 mL solution with initial ammonia concentration of 100 mg·L^{-1}, and adjusted pH = 9.0. The absorbance of the solution was determined by sampling every 1 h. After 10 h of reaction, the catalyst was recovered by centrifugation and used continuously for 7 times. The degradation curve is shown in **Figure 12**. At the 7th time, the ammonia nitrogen removal rate was still more than 85.5%. This shows that the NG/Bi_2S_3 catalyst is very stable. Gas chromatography analysis shows that the product of ammonia nitrogen degradation is nitrogen[24–26].

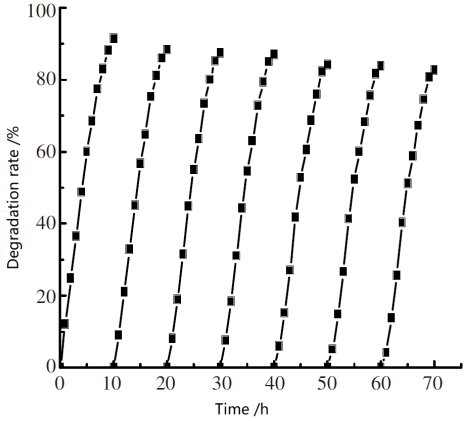

Figure 12. Catalyst recycling and stability.
Note: Degradation conditions: In near-infrared light, solution volume V = 50 mL, initial concentration of ammonia nitrogen C = 100 mg·L^{-1}, pH = 9.0, and mass of NG/Bi_2S_3 is 0.050 g.

4. Conclusion

NG/Bi_2S_3 composite photocatalyst was synthesized in one step by hydrothermal method. Using its narrow band gap, ammonia nitrogen in water was degraded by near-infrared light. The experiment results show that the photocatalytic activity of the composite catalytic material NG/Bi_2S_3 is higher than that of Bi_2S_3. When the initial concentration of ammonia nitrogen was 100.0 mg·L^{-1}, the pH value of the solution was 9.0, the amount of catalyst was 0.050 g, the loading amount of NG was 3 wt% and the near-infrared light was irradiated for 10 h, the efficiency of ammonia nitrogen degradation of NG/Bi_2S_3 composite reached 91.4%. The kinetic study shows that the degradation of ammonia nitrogen follows the first-order reaction kinetic law, and the average value of its apparent rate constant is 0.1240 h^{-1}.

Conflict of interest

The authors declare that they have no conflict of interest.

Acknowledgements

Foundation project: supported by the National Natural Science Foundation of China (21576175); Jiangsu Industry Foresight Project (BE2015190); graduate innovation project of Suzhou University of

Science and Technology (SKCX17_037).

References

1. Sivic A, Atanasova N, Puig S, *et al.* Ammonium removal in landfill leachate using SBR technology: Dispersed versus attached biomass. Water Science & Technology 2018; 77(1): 27–38.
2. Zhou Y, Xiao B, Liu S, *et al.* Photo-Fenton degradation of ammonia via a manganese-iron double-active component catalyst of graphene-manganese ferrite under visible light. Chemical Engineering Journal 2016; 283: 266–275.
3. Benáková A, Johanidesová I, Kelbich P, *et al.* The increase of process stability in removing ammonia nitrogen from wastewater. Water Science and Technology 2018; 77(9-10): 2213–2219.
4. Xiao S, Wang D, Zhang K, *et al.* Enhanced photoelectrocatalytic degradation of ammonia by in situ photoelectrogenerated active chlorine on TiO_2 nanotube electrodes. Journal of Environmental Sciences 2016; 50(12): 103–108.
5. Zhang M, He S, Tang W, *et al.* Disposal of low concentration ammonia-nitrogen wastewater using TiO_2/biochar composite. Research of Environmental Sciences 2017; 30(9): 1440–1447.
6. Chmielowski R, Pere D, Bera C, *et al.* Theoretical and experimental investigations of the thermoelectric properties of Bi_2S_3. Journal of Applied Physics 2015; 117(12): 125103.
7. Fang M, Jia H, He W, *et al.* Construction of flexible photoelectrochemical solar cells based on ordered nanostructural BiOI/Bi_2S_3 heterojunction films. Physical Chemistry Chemical Physics 2015; 17(20): 13531.
8. Li M, Wang J, Zhang P, *et al.* Superior adsorption and photoinduced carries transfer behaviors of dandelion-shaped Bi_2S_3@MoS_2: Experiments and theory. Scientific Reports 2017: 7: 42484.
9. Li Y, Fang X, Wang Y. Preparation of Bi_2S_3 micro/nano materials with various morphologies by hydrothermal method. Experimental Technology and Management 2017; 34(9): 47–51, 55.
10. Ilanthamizhan C, Manikandan A, Antony SA. Facile synthesis, structural, morphological and electrochemical properties of bismuth sulfide (Bi_2S_3) nanostructure. Journal of Nanoscience & Nanotechnology 2017; 17(2): 1193–1197.
11. Sharma S, Khare N. Synthesis of bismuth sulfide nanostructures for photodegradation of organic dye. Dae State Physics Symposium 2016; 2017; Odisha.
12. Cai A, Chang Y, Wang X, *et al.* Graphitic carbon nitride decorated with S, N co-doped graphene quantum dots for enhanced visible-light-driven photocatalysis. Journal of Alloys & Compounds 2017; 692: 183–189.
13. Peter CN, Anku WW, Sharma R, *et al*. N-doped ZnO/graphene oxide: A photostable photocatalyst for improved mineralization and photodegradation of organic dye under visible light. Ionics 2019; 25: 327–339.
14. Lin L, Nie Y, Kavadiya S, *et al.* N-doped reduced graphene oxide promoted nano TiO_2, as a bifunctional adsorbent/photocatalyst for CO_2, photoreduction: Effect of N species. Chemical Engineering Journal 2017; 316: 449–460.
15. Bu X, Yang S, Bu Y, *et al.* Highly active black TiO_2/N-doped graphene quantum dots nanocomposites for sunlight driven photocatalytic sewage treatmen. Chemistry Select 2018; 3(1): 201–206.
16. Zhang W, Zhang X, Dong X, *et al.* Synthesis of N-doped graphene oxide quantum dots with the internal P-N heterojunction and its photocatalytic performance under visible light illumination. Journal of Advanced Oxidation Technologies 2018; 21(1).
17. Liu S, Xiao B, Feng L, *et al.* Graphene oxide enhances the Fenton-like photocatalytic activity of nickel ferrite for degradation of dyes under visible light irradiation. Carbon 2013; 64(9): 197–206.
18. Zhou B, Shen A. Determination of ammonia nitrogen in water by Nessler reagent spectrophotometry. Low Carbon World 2017; 2017(8): 4.
19. Huang W, Xing C, Wang Y, *et al.* Facile fabrication and characterization of two-dimensional bismuth (III) sulfide nanosheets for high-performance photodetector applications under ambient conditions. Nanoscale 2018; 10(5): 2402–2412.
20. Yang C, Li Z, Yu Y, *et al.* Mesoporous zinc ferrite microsphere-decorated graphene oxide as a flame retardant additive: preparation, characterization, and flame retardance evaluation. Industrial & Engineering

Chemistry Research 2017; 56(27): 7720–7729.
21. Hsieh C, Liu W. Synthesis and characterization of nitrogen-doped graphene nanosheets/copper composite film for thermal dissipation. Carbon 2017; 118: 1–7.
22. Baishya K, Ray JS, Dutta P, *et al.* Graphene-mediated band gap engineering of WO_3 nanoparticle and a relook at Tauc equation for band gap evaluation. Applied Physics A 2018; 124(10): 1–6.
23. Yang H, Yao R. Effects of pH level and nitrifying bacteria concentration on ammonia oxidation rate. Chinese Journal of Environmental Engineering 2017; 11(5): 2660–2665.
24. Zhou S, Xiao B, Liu C, *et al.* Photocatalytic degradation of ammonia via graphene oxide-nickel ferrite hybrid catalyst under visible light irradiation. Journal of Suzhou University of Science and Technology (Natural Science Edition) 2016; 33(2): 23–29.
25. Liu S, Zhu X, Zhou Y, *et al.* Smart photocatalytic removal of ammonia through molecular recognition of zinc ferrite/reduced graphene oxide hybrid catalyst under visible-light irradiation. Catalysis Science & Technology 2017; 7(15): 3210–3219.
26. Xue T, Zhang H, Liu S. Synthesis of reduced graphene oxide-cerium oxide hybrid catalyst and the degradation of ammonia under visible light irradiation. Journal of Functional Materials 2017; 48(3): 3218–3222.